Marcin Madej[1]*, Beata Leszczyńska-Madej[2], Anna Wąsik[2], Anna Kopeć-Surzyn[1], Patryk Korban[2], Dariusz Garbiec[3]

[1] AGH – University of Science and Technology, Faculty of Metals Engineering and Industrial Computer Science, al. A. Mickiewicza 30, 30-059 Krakow, Poland
[2] AGH –University of Science and Technology, Faculty of Non-Ferrous Metals, al. A. Mickiewicza 30, 30-059 Krakow, Poland
[3] Łukasiewicz Research Network – Poznań Institute of Technology, ul. E. Estkowskiego 6, 61-755 Poznan, Poland
*Corresponding author. E-mail: mmadej@agh.edu.pl

EFFECT OF PRODUCTION PROCESS PARAMETERS ON DENSIFICATION, MICROSTRUCTURE AND SELECTED PROPERTIES OF SPARK PLASMA SINTERED Al4Cu-xSiC COMPOSITES

The paper presents the results of a study on the microstructure and hardness measurements of Al4Cu-xSiC (x = 5, 10, 20 and 30 wt.%) composites produced by spark plasma sintering (SPS). The sintering process was carried out in an HP D 25/3 plasma sintering furnace in a vacuum atmosphere, with sintering temperatures of 580 and 600°C and a densification pressure of 50 MPa. The heating rate was 100°C/min and the isothermal holding time at the sintering temperature was 2.5 min. As a reference material, the AlCu matrix was sintered under the same conditions. As a result, composites with a near-full density of 96.5-99.5% were obtained. Microstructure studies were performed employing the techniques of light microscopy, scanning, and transmission electron microscopy, along with analysis of the chemical composition in microareas. The test results did not reveal remarkable differences in the microstructure of the investigated composites sintered at 580 and 600°C. The sinters have a fine-grained microstructure with a strengthening phase located at the grain boundaries; locally, pores are visible. Increasing the SiC content in the composites promotes the formation of agglomerates of these particles. It was proven that a higher sintering temperature has a positive effect on the hardness of the studied composites.

Keywords: AlCu-SiC composites, SPS, silicon carbide, microstructure

INTRODUCTION

Particulate silicon carbide reinforced aluminium matrix composites have aroused considerable interest in applications in the automobile and aerospace industries as advanced engineered materials due to their low density, as well as excellent mechanical, chemical and electrical properties [1-3].

Powder metallurgy is one of the fabrication techniques for metal matrix composites, which involves mixing ceramic particles with metal powder, compaction and a sintering process, allowing composites to be obtained with a homogeneous distribution of the reinforcing phase and excellent properties as the manufacturing process is not influenced by the wettability of the ceramic particles and the metal matrix [4]. The compaction of ceramic particles by the traditional sintering process involves high sintering temperatures and a long holding time [5], which is associated with a risk of the formation of coarse-grained material with insufficient mechanical properties [6]. Spark plasma sintering (SPS) is a more efficient sintering technique, capable of obtaining fully dense metal-ceramic composite materials with strong interfacial bonding and a clean interface [7, 8]. This sintering technique provides a high heating rate, a short holding time at a lower process temperature, and rapid densification kinetics [9, 10]. In SPS, powder materials are consolidated by simultaneous heating by means of a direct electric current and compression [11]. Strong adhesion bonds between the sintered particles are formed as a result of electrical discharge and spark generation, which results in breaking the oxide film in the metal powders, neck growth, and diffusion enhancement. Running the process fast at temperatures below the melting point of the metal allows detrimental interface reactions to be controlled [12, 13].

Many authors have applied the SPS technique to synthesise Al-SiC composites. Farzaneh Jafari et al. [14] indicated that the implementation of SPS in the fabrication of Al-SiC composites allowed the acquisition of a significantly higher density and hardness, and thus a lower wear rate of the produced materials compared to those obtained by the conventional manufacturing method. Yu Hong et al. [15] investigated the influence of the SPS parameters and the size of the SiC particles on the thermal-mechanical properties of 6061Al-50vol.% SiC composites. Five different sintering temperatures (500, 520, 540, 560 and 580°C) were applied. Higher densification (99.8 %) and bending strength (649 MPa) were achieved after sintering at 520°C and no reaction products were observed at the Al-SiC interface. Ismaila Kayode Aliyu et al. [16] determined the influence of the

SPS parameters on the microstructure and properties of an aluminium matrix reinforced with 1 wt.% SiC nanoparticles. The authors observed a greater effect of the applied pressure and sintering temperature than the heating rate or sintering time on the density, compressive strength, and microhardness of the studied materials. Jiang-Tao Zhang et al. [17] also indicated a significant effect of the SPS parameters on the consolidation of Al-SiC composites. Zhao-Hui Zhang et al. [18] investigated the mechanical properties of Al-SiC composites sintered at different temperatures. The application of the SPS method allowed a composite material to be obtained with a relative density of 99.6%, a microhardness of 25.5 GPa and a bending strength of 451 MPa. Sivaiah Bathula et al. [19] successfully synthesised Al5083-SiC nanocomposites using the SPS technique with a clear and free intermetallic interface.

The aim of this study is to examine the possibility of producing composites on an Al4Cu matrix reinforced with SiC particles using the SPS method and to determine the microstructure and hardness depending on the process parameters. Studies on the manufacture of composites based on an aluminium matrix and reinforced with SiC particles have yielded positive results; therefore, it was decided to make composites with the same SiC content, but based on the Al4Cu alloy matrix [20]. The microstructure and final properties of metal matrix composites are affected by the sintering process. A properly conducted sintering process has a decisive influence on the durability of the matrix-reinforcement interface as the effective external stress transfer is influenced by the interfacial adhesion between the metal and ceramic particles. However, the sintering of metal-ceramic systems brings difficulty in obtaining the proper connection quality of the component due to the difference in thermal expansion coefficients between the metal matrix and the ceramic reinforcement. In the conducted research, an attempt was made to obtain high quality metal-ceramic bonds in Al4Cu-SiC composites by applying the SPS method and examine the influence of SPS on the microstructure and mechanical properties

of the investigated materials. The choice of SPS to sinter the Al4Cu-SiC composites was motivated by the fact that the sintering of aluminium and its alloys is hindered because of its high affinity for oxygen. As a result, the aluminium powders are covered with a thin layer of oxides, which is a barrier to the formation of diffusion bonds between the particles. During SPS, spark discharges can be generated in the gaps between the powder particles, which favour the evaporation of oxides because of the local temperature increase on the powder surfaces and facilitates effective bonding between the aluminium particles.

MATERIALS AND METHODS

The powders used in the study were Al grade 1070 (Benda Lutz, Skawina, Poland), with a particle size of less than 63 μm, electrolytic copper powder (Euromet, Trzebinia, Poland) with a particle size of less than 40 μm and SiC powder (Alfa Aesar) with a particle size of less than 2 μm. The aluminium powder contains the following fractions: above 63 μm – 5%, in the range of 32-63 μm – 45-70%, the rest – below 32 μm. The copper powder consisted of the following fractions: below 10 μm – 10%, in the range of 10-25 μm – 85%, the rest in the range 25-40 μm.

The following mixtures were prepared from the powders:
- Al + 4 wt.%Cu
- Al + 4 wt.%Cu + 5 wt.%SiC
- Al + 4 wt.%Cu + 10 wt.%SiC
- Al + 4 wt.%Cu + 20 wt.%SiC
- Al + 4 wt.%Cu + 30 wt.%SiC.

The powder mixtures were prepared in a Turbula T2F type mixer. The mixing time was 30 min. The morphology of the Al powder particles is shown in Figure 1a, the Cu powder particles in Figure 1b, and the SiC powder particles in Figure 1c, the powder mixture of Al4Cu+20wt.%SiC after mixing in the Turbula T2F mixer in Figures 1d-f.
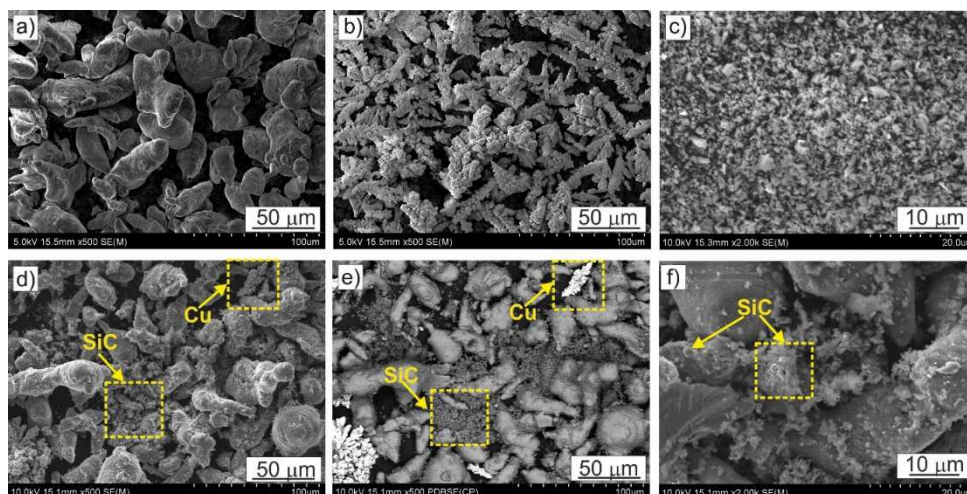

Fig. 1. Morphology of initial powders: a) aluminium, b) copper, c) SiC, d-f) powder mixture of Al4Cu + 20 wt.%SiC after mixing in Turbula T2F mixer; SEM

The sintering process was performed using an HP D 25-3 furnace (FCT Systeme GmbH). For this purpose, tools made from 2333 graphite were utilised (MERSEN). The loading chamber in the graphite tool unit was filled with the powder mixture. For technological reasons, Papyex N998 graphite film (MERSEN) was placed between the powder mixture and the die and punches. Next, the tools were placed in the sintering chamber of the HP D 25-3 furnace to perform the sintering process, which was carried out in a vacuum, at the sintering temperatures of 580 and 600°C, respectively, and under the compaction pressure of 50 MPa. The heating rate was 100°C/min, and the sintering time was 2.5 min. The duration of a single current impulse was equal to 125 ms, and the interval between the impulses lasted 5 ms. Samples with dimensions of Ø40 x10 mm were produced. The density of the sinters was determined by the Archimedes method. Microstructure studies were carried out by means of an Olympus GX 51 light microscope (LM) and scanning electron microscope (SEM) Hitachi SU 70. Photographs were taken during the operation of the detector, collecting secondary scattered electrons SE or backscattered electrons BSE. In addition, elemental distribution maps were made employing energy-dispersive X-ray scattering (EDS). Microstructure observations of the samples in the submicron range were conducted utilising a JEM-2010 ARP transmission electron microscope (TEM) (JEOL). The samples for observation were produced by the ionic thinning method using a PIPS device (Gatan). Hardness measurements were performed by means of the Brinell method. A carbide ball with a diameter of 2.5 mm was used and measurements were made with a load of 62.5 kG. Each sample was measured at five random locations with a distance of at least two indentation diameters between the indentations.

RESULTS AND DISCUSSION

The relative densities of the composites were determined on the basis of the real density measured by the Archimedes method and the theoretical density determined from the mixing rule, which is an approximate result. The estimated relative densities are closely dependent on the chemical composition mixture of the researched composites and are a function of the sintering temperature. A slight increase in the sintering temperature, by only 20°C, results in an increment in the final density of the sinters, but they are generally rises of about ±0.2-0.4% (Fig. 2). It can be assumed that 580°C is the optimum sintering temperature for composites with a higher silicon carbide content. It was also observed that increasing the content of the reinforcing phase has a positive effect on the final density of the composites, despite the fact that its hardness hinders compaction due to pressure effects during sintering. It can be assumed that the increased content of silicon carbide reduces the disadvantageous effect of the addition of copper (whose proportion in the total volume of

the sinter decreases) on the sintering process. SPS is associated with the flow of electrical pulses through the volume of the powder mixture, and the good electrical and thermal conductivity of copper results in a reduction in the effectiveness of their interaction at the contact boundaries, where it occurs until it diffuses into the aluminium.

Micrographs of the microstructure of the studied materials are shown below, which confirm the obtained density results. The observations indicate a very small proportion of pores in the volume of the sinters, irrespective of the observation location. The pores are mainly located at the grain boundaries, probably where the copper powder particles are present. This is confirmed by observation of the microstructure of the Al4Cu sinter (Fig. 3a, c), in which the highest proportion of pores was revealed.
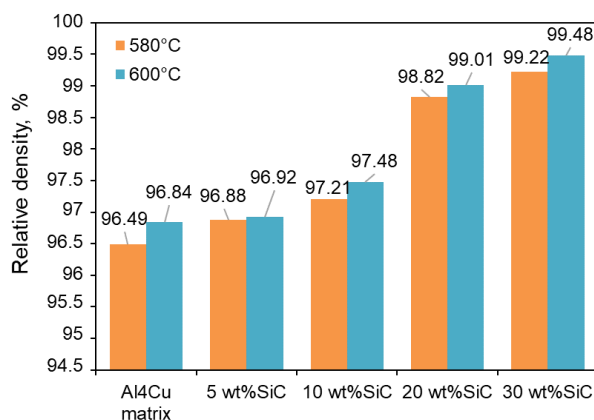

Fig. 2. Relative densities of Al4Cu-xSiC (x = 5, 10, 20, 30 wt.%) composites depending on SiC content and sintering temperature

A characteristic feature of the microstructure of the Al4Cu matrix, both sintered at 580 and 600°C, are regular grains with well-defined boundaries (Fig. 3). In addition, individual pores are visible, which are located at the grain boundaries. No individual copper particle precipitates or large precipitates of the Al_2Cu phase were found at the grain boundaries or inside the grains, suggesting that the copper is mainly in solution. This can be confirmed by the results of the point analysis shown in Figures 4 and 5. This implies that during the SPS process there are no conditions that favour the precipitation of the Al_2Cu phase. The amount of copper in the matrix does not exceed 3.7 wt.%. The obtained results demonstrate the presence of Al_2O_3 aluminium oxide particles at the grain boundaries. The presence of Al_2O_3 at the grain boundaries is related to the fact that aluminium is a metal with a high affinity for oxygen; the oxide film that covers the powder is already formed at the manufacturing process stage and grows during both transport and storage of the powder. Under the pressure and temperature conditions of the SPS process, this layer breaks down, allowing permanent bonding between the powder particles. In addition, the fine Al_2O_3 particles provide additional reinforcement to the material.
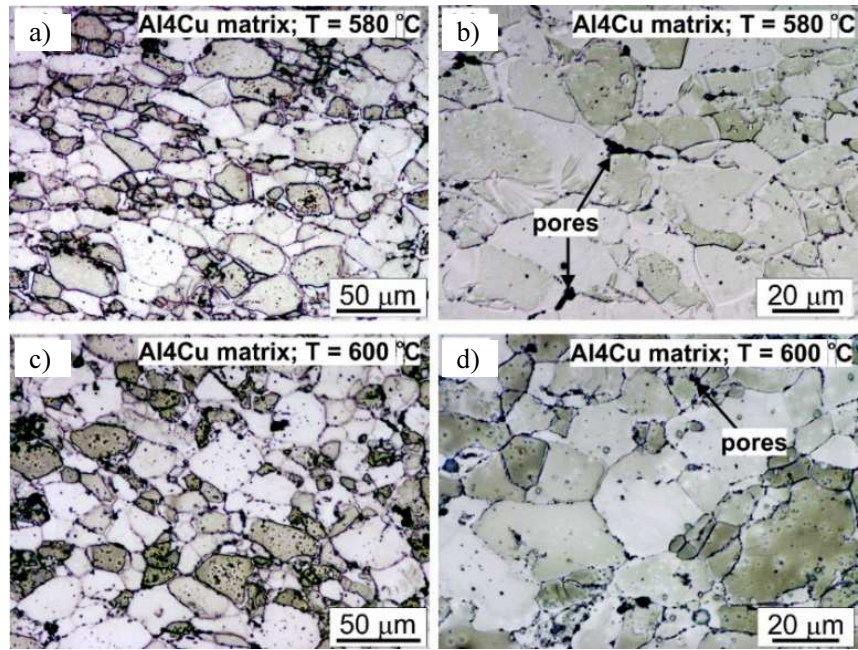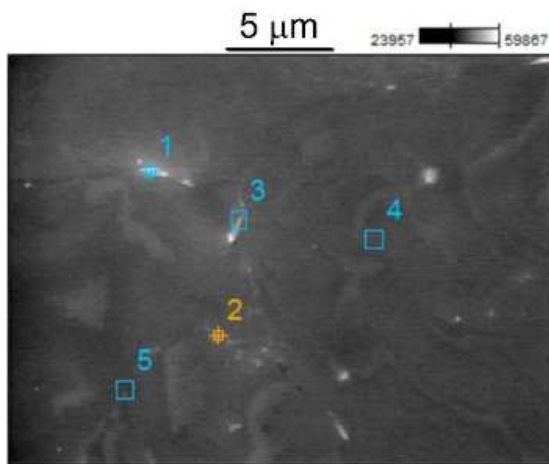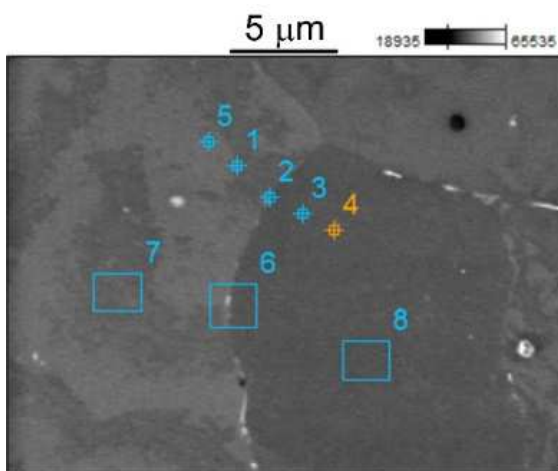
Fig. 3. Microstructure of spark plasma sintered Al4Cu matrix; a-b) T = 580°C, c-d) T = 600°C; LM

wt%	Al	Cu	O
1	95.5	3.2	1.3
2	96.7	2.6	0.7
3	96.4	3.2	0.4
4	96.9	2.7	0.4
5	97.1	2.6	0.3

Fig. 4. SEM and corresponding EDS mapping micrographs of Al4Cu matrix spark plasma sintered at T = 580°C

wt%	Al	Cu
1	96.4	3.6
2	97.2	2.8
3	96.5	3.5
4	96.6	3.4
5	96.6	3.4
6	96.3	3.7
7	96.9	3.1
8	96.5	3.5

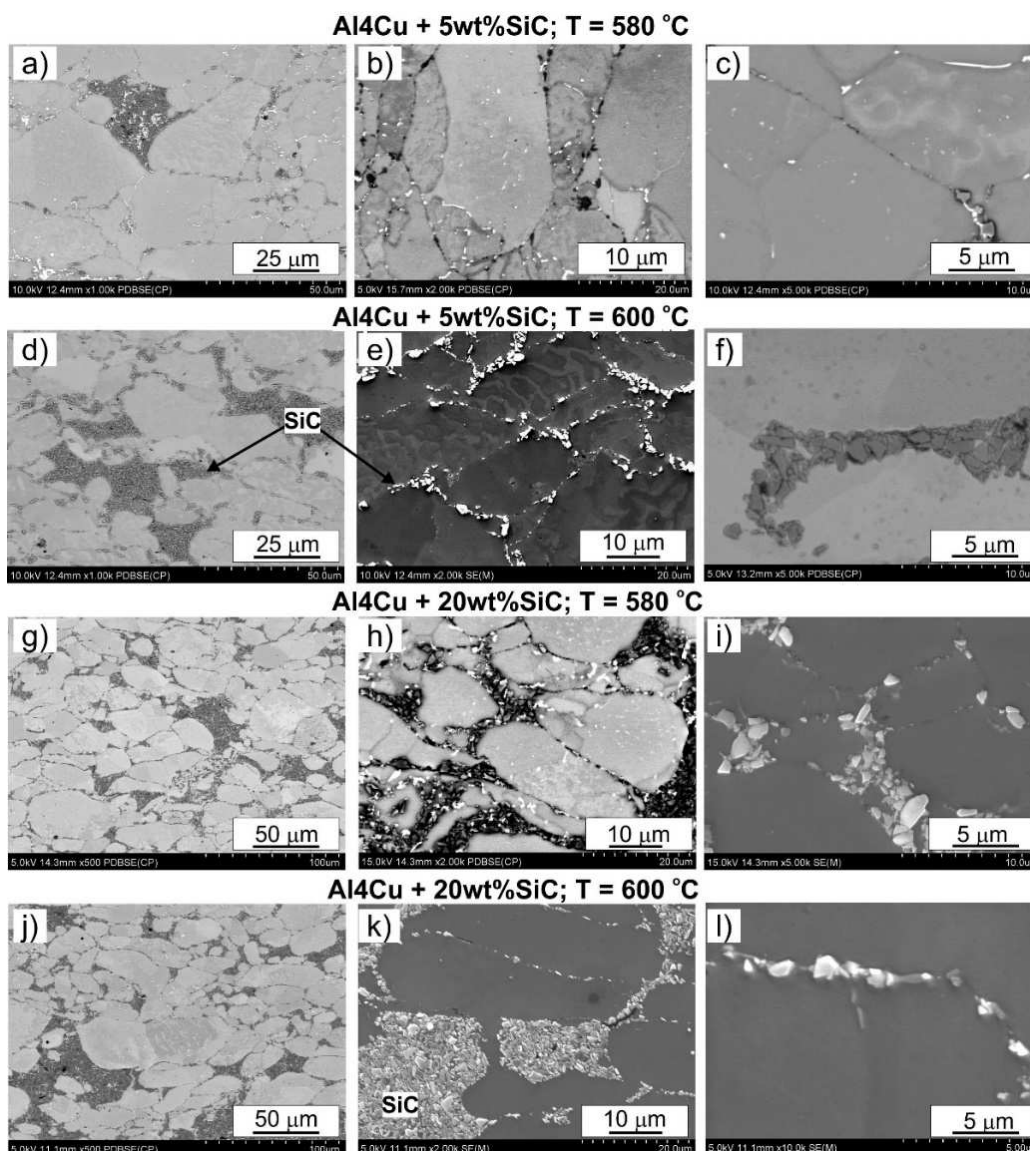Fig. 5. SEM and corresponding EDS mapping micrographs of Al4Cu matrix spark plasma sintered at T = 600°C

Fig. 6. Microstructure of spark plasma sintered Al4Cu-xSiC composites; a-c) Al4Cu + 5 wt.%SiC, T = 580°C, d-f) Al4Cu + 5 wt.%SiC, T = 600°C, g-i) Al4Cu + 20 wt.%SiC, T = 580°C, j-l) Al4Cu + 20 wt.%SiC, T = 600°C; SEM

The microstructure of the composites sintered at 580°C and 600°C shows no significant differences. In both the 580°C and 600°C sintered composites, the reinforcing phase is located at the grain boundaries (Figs. 6-8). Raising the content of the SiC-reinforcing phase favours the formation of agglomerates. The phenomenon of SiC particle clusters is also favoured by the large variation in particle sizes of Al, Cu (< 63μm) and SiC (< 2μm). Mixing in the Turbula T2F mixer did not allow fully uniform distribution of the SiC particles in the matrix. The micrographs shown in Figures 6c, f, i, l, taken at high magnification and showing the contact boundary between the matrix and the SiC particles, indicate a good bond between the components, with no discontinuities or pores found, even in the area of the SiC particle clusters. Fine pores are located at the grain boundaries, particularly evident in the composites sintered at the lower temperature of 580°C (Fig. 6b). Cu-rich precipitates (probably the Al_2Cu phase) were also found at the grain boundaries and in the area of SiC

agglomerates, and locally also within the grains, as can be seen in Figures 7 and 8 showing maps of elemental distribution in the micro-areas. The presence of silicon carbide favours precipitate formation, probably because of changes in the heat transport conditions inside such materials. The presence of Al_2O_3 oxides, which form a regular lattice at the grain boundaries, was also demonstrated (Fig. 8).

To more fully verify the microstructure of the studied composites, observations were made for selected variants using transmission electron microscopy (TEM). A characteristic feature of the substructure of the investigated materials are the subgrains present in the matrix material region (Fig. 9). The size of the subgrains is less than 1 μm. Locally, dislocations that form low-energy systems are observed, as well as clusters of Al_2O_3 (Fig. 9d). The size of individual Al_2O_3 particles does not exceed several tens of nanometres. The conducted studies proved good bonding at the matrix-SiC interface (Fig. 9c). There is an

increased amount of dislocation in the bonding area with the ceramic phase. In addition, fine pores were found to be locally present at the grain boundaries of the matrix, forming a lattice (Fig. 9b). The presence of pores at the boundaries of the lattice is unfavourable, especially when there are many of them, as it reduces fracture toughness and deteriorates the strength properties.
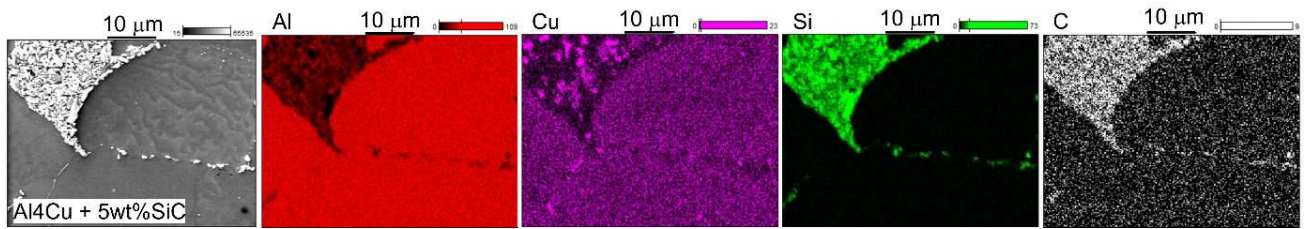

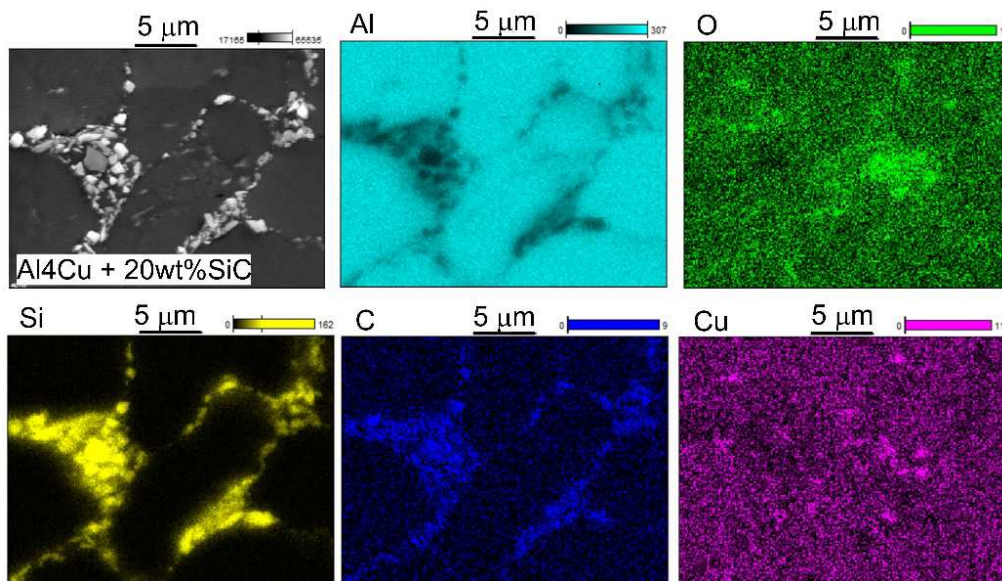Fig. 7. SEM and corresponding EDS mapping micrographs of Al4Cu + 5 wt.%SiC composite spark plasma sintered at T = 580°C

Fig. 8. SEM and corresponding EDS mapping micrographs of Al4Cu + 20 wt.%SiC composite spark plasma sintered at T = 600°C
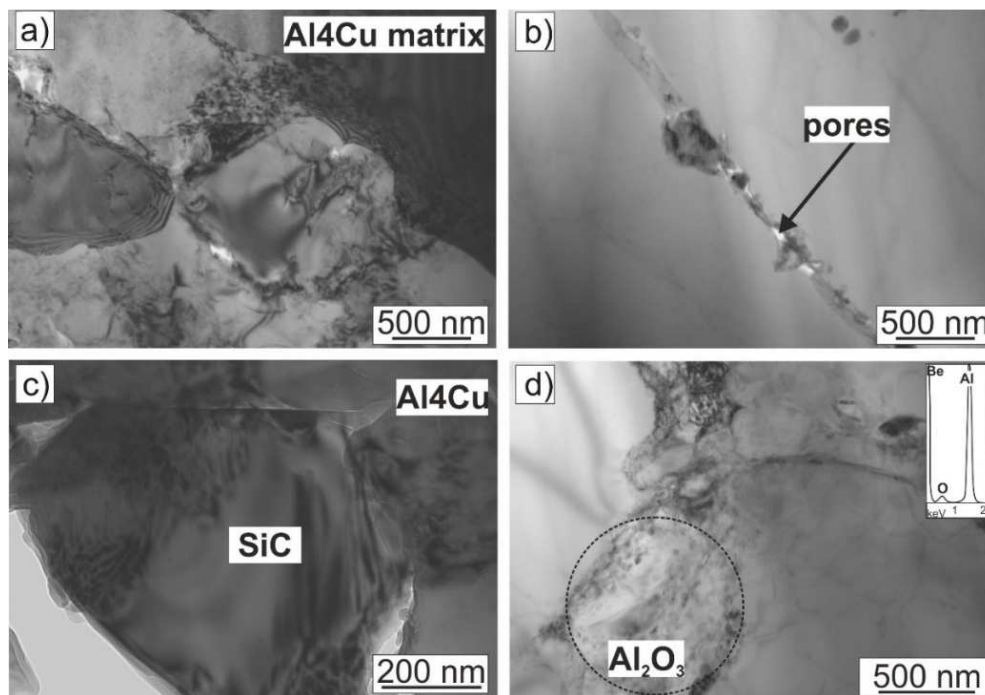

Fig. 9. Microstructure of spark plasma sintered: (a, b) Al4Cu matrix (c, d) and Al4Cu + 5 wt.%SiC composite as well as spectrum from chemical composition analysis from Al_2O_3 area; T = 600°C, TEM
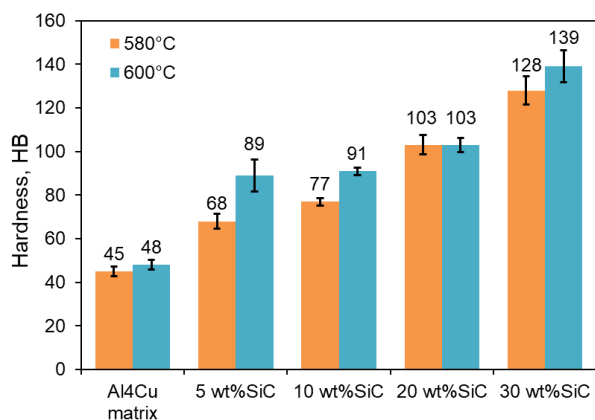
Fig. 10. Hardness of spark plasma sintered Al4Cu-xSiC (x = 5, 10, 20, 30 wt.%) composites depending on SiC content and sintering temperature

The results of the Brinell hardness measurements presented in Figure 10 confirmed the beneficial effect of the addition of silicon carbide. A favourable effect of increasing the sintering temperature on the obtained results can also be indicated. The hardness of the matrix itself (45-48 HB) is significantly higher than that of pure aluminium, indicating that, despite the short time of exposure to temperature, copper diffuses into the aluminium and causes its strengthening. Nonetheless, no precipitation of the Al$_2$Cu phase was observed. The main factor determining the hardness is the proportion and distribution of the strengthening SiC phase against the matrix. With a minimum of 70% plastic content of the matrix in the composites, the increase in hardness is only about threefold, indicating that the hardness in this type of material depends more strongly on the plastic factor in the chemical composition. The maximum hardness obtained for the composites with the 30% SiC content is about 140 HB. A solution could be to reduce the size of the SiC particles and distribute them evenly in the matrix by milling them in a ball mill; however, in reality the fine particles tend to form permanent agglomerates that do not break down in a Turbula-type mixer and are present in the microstructure of the finished materials, weakening them.

CONCLUSION

The following conclusions were drawn from the study:
– The density of the composites strictly depends on the parameters of the SPS manufacturing process and the chemical composition of the researched composites. It grows with increasing content of the reinforcing phase in the form of SiC carbide.
– The addition of silicon carbide has a favourable effect on the hardness of the studied composites, which is due to its properties and good cohesion both with the matrix and between adjacent SiC particles.

– The employed manufacturing process parameters appear to be optimal, especially for the composites with a high silicon carbide content (20 and 30%).
– The addition of copper in the form of an elementary powder hinders the sintering process by the SPS method in contrast to materials produced in the classical manner; this influence is compensated by increasing the proportion of the reinforcing phase.

Acknowledgement

REFERENCES

[1] Erdemir F., Canakci A., Varol T., Corrosion and wear behavior of functionally graded Al2024/SiC composites produced by hot pressing and consolidation, Journal of Alloys and Compounds 2015, 644, 589-596, DOI: 10.1007/s12633-021-01582-7.

[2] El-Gallab M., Sklad M., Machining of Al/SiC particulate metal matrix composites: Part II: Workpiece surface integrity, Journal of Materials Processing Technology 1998, 83(1-3), 277-285, DOI: 10.1016/S0924-0136(98)00072-7.

[3] Çevik Z.A., Karabacak A.H., Kök M., Canakçı A., Kumar S.S., Varol T., The effect of machining processes on the physical and surface characteristics of AA2024-B4C-SiC hybrid nanocomposites fabricated by hot pressing method, Journal of Composite Materials 2021, 55(19), 2657-2671, DOI: 10.1177/0021998321996419.

[4] Ogawa F., Masuda C., Microstructure evolution during fabrication and microstructure-property relationships in vapour-grown carbon nanofibre-reinforced aluminium matrix composites fabricated via powder metallurgy, Composites Part A 5015, 71, 84-94, DOI: 10.1016/j.compositesa.2015.01.005.

[5] Castillo-Rodríguez M., Munoz A., Domíngguez-Rodríguez A., Effect of atmosphere and sintering time on the microstructure and mechanical properties at high temperatures of [alpha]-Sic sintered with liquid phase Y$_2$O$_3$-Al$_2$O$_3$, Journal of the European Ceramic Society 2006, 26, 12, 2397-2405, DOI: 10.1016/j.jeurceramsoc.2005.04.018.

[6] Saha S., Ghosh M., Kumar Pramanick A., Mondal Ch., Maity J., Microstructure and mechanical properties of Al/Cup/SiCp/ TiCp-based hybrid composites fabricated by spark plasma sintering, Journal of Materials Engineering and Performance 2022, 31, 424-438, DOI: 10.1007/s11665-021-06164-7.

[7] Haque A., Shekhar S., Murty S., Ramkumar J., Fabrication of controlled expansion Al-Si composites by pressureless and spark plasma sintering, Advanced Powder Technology 2018, 29, 3427-3439, DOI: 10.1016/j.apt.2018.09.024.

[8] Mizuuchi K., Inoue K., Agari Y., Nagaoka T., Sugioka M., Manaka M., Takeuchi T., J.-Tani J., Kawahara M., Makino Y., Ito M., Processing of Al/SiC composites in continuous solid-liquid co-existent state by SPS and their thermal properties, Composites Part B: Engineering 2012, 43, 2012-2019, DOI: 10.1016/j.compositesb.2012.02.004.

[9] Kang P., Zhao Q., Guo S., Xue W., Liu H., Chao Z, Jiang L., Wu G., Optimisation of the spark plasma sintering process for high volume fraction SiCp/Al composites by orthogonal experimental design, Ceramics International 2021, 47, 3816-3825, DOI: 10.1016/j.ceramint.2020.09.240.

[10] Li XP., Liu CY., Ma MZ., Liu RP., Microstructures and mechanical properties of AA6061-SiC composites prepared through spark plasma sintering and hot rolling, Materials Science & Engineering A 2016, 650, 139-144, DOI: 10.1016/j.msea.2015.10.015.

[11] Ujah Chika O., Aigbodion VS., Ezema Ike-Eze Ikechukwu Ch., Makhatha Mamookho E., Spark plasma sintering of aluminium composites – a review, The International Journal of Advanced Manufacturing Technology 2021, 112, 1819--1839, DOI: 10.1007/s00170-020-06480-7.

[12] Xiaofeng G., Liamneng Z., Dongming Z., Meijun Y., Zezhong W., Spark Effect on the densification of SiCp/Al composites by SPS, Journal of Wuhan University of Technology-Mater. Sci. Ed. 2006, 21, 1, 72-75.

[13] Cobbinah P.V., Matizamhuka W.R., The efect of SiC content on the tribocorrosion performance of spark plasma sintered Al-SiC nanocomposites, SN Applied Sciences 2019, 1, 1679, DOI: 10.1007/s42452-019-1770-z.

[14] Jafari F., Sharifi H., Reza Saeri M., Tayebi M., Effect of reinforcement volume fraction on the wear behavior of Al-SiCp composites prepared by spark plasma sintering, Silicon 2018, 10, 2473-2481, DOI: 10.1007/s12633-018-9779-2.

[15] Hong Y., Liu J., Wu Y., The interface reaction of SiC/Al composites by spark plasma sintering, Journal of Alloys and Compounds 2023, 949, 169895, DOI: 10.1016/j.jallcom.2023.169895.

[16] Aliyu I.K., Saheb N., Hassan S.F., Al-Aqeeli N., Microstructure and properties of spark plasma sintered aluminum containing 1 wt.% SiC nanoparticles, Metals 2015, 5, 70-83, DOI: 10.3390/met5010070.

[17] Zhang JT., Liu LS., Zhai PCh., Fu ZY., Zhang QJ., Effect of fabrication process on the microstructure and dynamic compressive properties of SiCp/Al composites fabricated by spark plasma sintering, Materials Letters 2008, 62, 3, 443--446, DOI: 10.1016/j.matlet.2007.04.118.

[18] Zhang ZH., Wang FCh., Luo J., Lee SK., Wang L., Microstructures and mechanical properties of spark plasma sintered Al-SiC composites containing high volume fraction of SiC, Materials Science and Engineering A 2010, 527, 7235--7240, DOI: 10.1016/j.msea.2010.07.043.

[19] Bathula S., Anandani RC., Dhar A., Srivastava AK., Microstructural features and mechanical properties of Al 5083/SiCp metal matrix nanocomposites produced by high energy ball milling and spark plasma sintering, Materials Science and Engineering: A 2012, 545, 30, 97-102, DOI: 10.1016/j.msea.2012.02.095.

[20] Leszczyńska-Madej B., Garbiec D., Madej M., Effect of sintering temperature on microstructure and selected properties of spark plasma sintered Al-SiC composites, Vacuum 2019, 164, 250-255, DOI: 10.1016/j.vacuum.2019.03.033.